

## EFFORTS ON NONDESTRUCTIVE INSPECTIONS FOR SC CAVITIES

Y. Iwashita, Y. Fuwa, M. Hashida, S. Sakabe, S. Tokita, H. Tongu, Kyoto ICR, Uji, Kyoto, Japan  
 K. Otani, INRS-EMT, Varennes, Québec, Canada  
 H. Hayano, K. Watanabe, Y. Yamamoto, KEK, Ibaraki, Japan

### Abstract

Efforts on nondestructive inspections for SC cavities are reported. The high resolution T-map, X-map system is designed so that the installation time of the mapping system can be reduced. It also reduces the number of cables for the signal transmission and the number of pins of the vacuum feed-through. Zr K-shell X-ray seems a good candidate for the radiography technique for the defects buried under the Nb cavity surface. The local repairing technique using the micro-grinder is also reported, which is used after a defect is identified and located through the inspections.

### INTRODUCTION

The high resolution camera, so-called Kyoto Camera, inspecting the superconducting (SC) cavity inner surface showed the importance of nondestructive inspections to improve yield in production of high performance SC Cavities [1]. Further efforts have been continued for the inspection and the high resolution T-map, X-map and eddy current scanner have been developed [2, 3, 4, 5, 6]. Use of radiography to detect small voids inside the Nb EBW seam with the target resolution of 0.1 mm is under investigation. We have carried out radiography tests with X-rays induced from an ultra-short pulse intense laser. The local repairing technique can be employed when they indicate a need of treatments. These techniques improved the production yield of the SC cavities.

### HIGH RESOLUTION T-MAP, X-MAP

The temperature mapping (T-map) and X-ray mapping (X-map) for inspections for SC accelerator cavities are under development. Among various X-map and T-map methods, our XT-map system (mixed system of X-map and T-map) has following features.

- Spatially high-resolution
- Reduction of number of wiring signal cables
- Easy installation
- Use of low-cost components available on market

Figure 1 shows the block diagram of T-map part. The reduction of number of wiring signal cables is achieved by signal multiplexers at the cryogenic area, which also reduces LqHe consumption (see Fig. 1 and Fig. 2). The X-map part has a similar configuration but with less number of sensors. The sensors are mounted on flexible printed circuit sheets, which are stretched on a cavity surface with the chip resistor face down (see Fig. 3 and Fig. 4). Appropriate tensions keep enough contact pressure for good thermal contacts. This wrapping up technique makes the sensor installation process at the

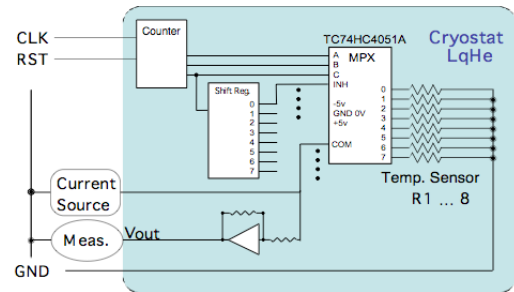


Figure 1: Block diagram of T-map part.

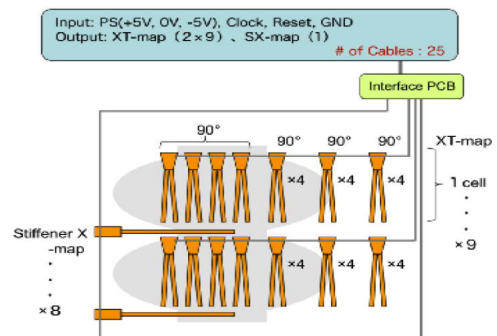


Figure 2: The inter-connection for the XT-map system.

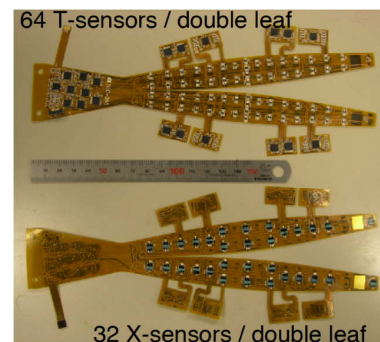


Figure 3: Leaf shaped flexible PCB.

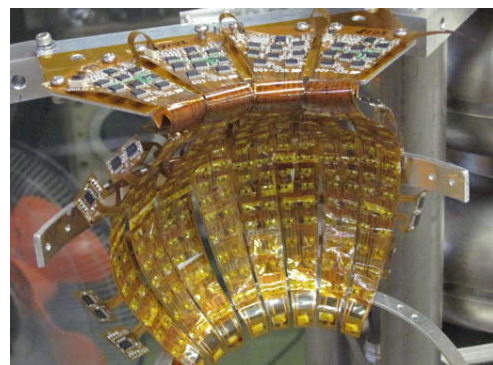


Figure 4: Chip resistors are mounted on inner side.

preparation of vertical test easy (see Fig. 5). Instead of conventional (legacy) carbon resistors (such as made by Allen Bradley), chip resistors for SMT (Surface Mount Technology) are used as temperature sensors. We confirmed that RuO<sub>2</sub> type chip resistors have enough sensitivity around 4 K. Thin polyimide sheets insulate the chip resistors from a cavity surface. One temperature sensor covers about 1cm<sup>2</sup> except iris zone which is not accessible for the sensors from a cavity outer surface.

X-ray sensors (PIN-photo diodes) are mounted on the other side of the chip resistors (outer side) to make better use of the limited surface area of the PCB. Only 25 cabling wires should handle the all sensors (1024 T-sensors/cell x 9 cells + 512 X-sensors/cell x 9 cells = 13824 signals). Although X-rays are mostly anticipated at the iris zone, the accessibility is not good because of the stiffer ring. Stiffer X-map system is developed so that X-sensors on a strip sheet can slip in under the stiffer ring (see Fig. 6 and Fig. 7). This configuration reduces the attenuation of X-rays emitted from the iris zone passing through the Nb material.

A preliminary quench detection test for the XT-map system was carried out during one of regular vertical tests at KEK. Four sets of double leaves were placed on a quenched location where was identified by a previous vertical test as shown in Fig. 8. It covers a 1/4 part (90 degrees) of a cell. Figure 8 Left shows a measured result of T-map test with a heater (26W). Temperature rise caused by the heater put on the cavity was detected. Figure 8 Right shows a result of actual quench. Local temperature rises were successfully detected at the previously quenched location. Since some sensors may have poor thermal contacts, not all the observed temperature rise signals in this first preliminary test may be real. Particularly, the contacts at the equator region need more care, since the surfaces of EBW seams are not flat in addition to the grooves (thinner Nb thickness) machined for the EBW.



Figure 5: Installed XT-map leaves on a cell. X-sensors are mounted on outer side. Multiplexers, peripherals and connections are on the base of the leaves.



Figure 6: Stiffener X-map.

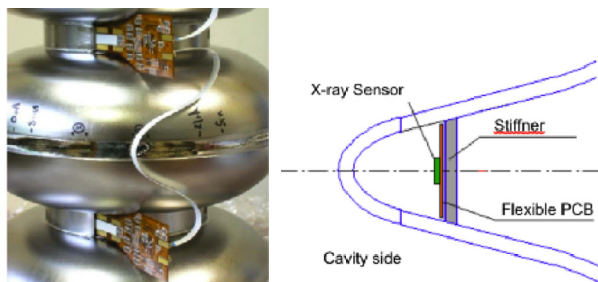


Figure 7: Installed stiffener X-map ribbons. The ribbons go under the stiffer ring.

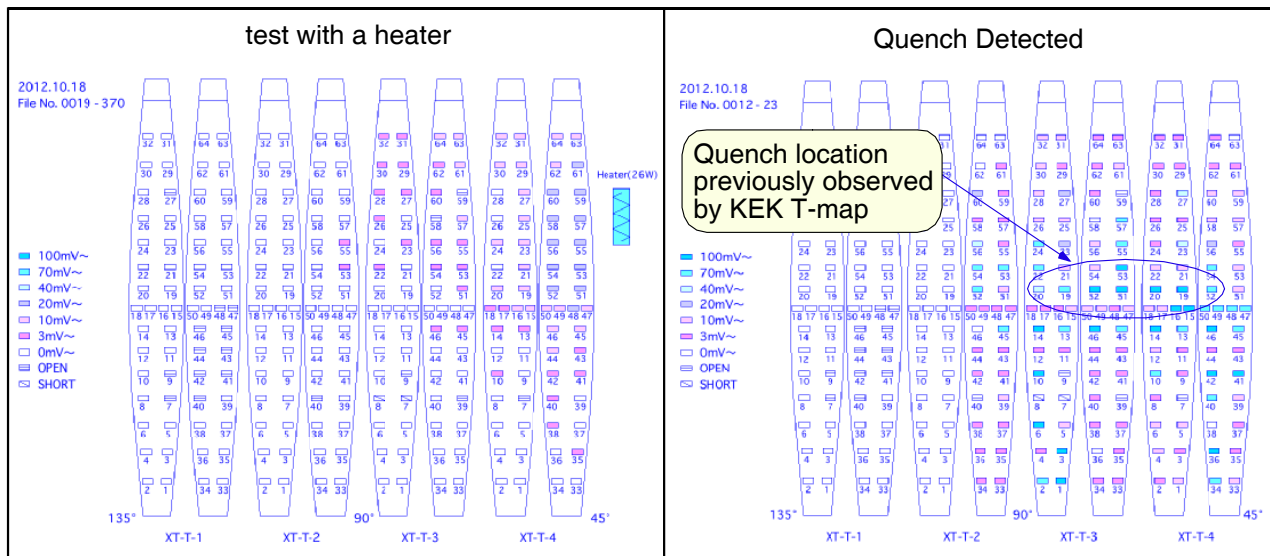


Figure 8: Detection test of T-map. Left: initial test with a heater. Right: Quench detected at the vicinity of the location previously identified by the KEK system. 100mV corresponds to temperature rise from 2K to 10K.

## RADIOGRAPHY

Recently, defects or voids buried under the Nb material surface need to be paid attention. Various radiography techniques have been investigated such as X-ray CT, and neutron CT. The larger atomic number of Nb highly attenuates X-rays. The higher the energy of X-rays, the better the transmission through materials. The contrast, however, becomes worse at the higher energy. Although the phase contrast techniques should have better contrast, it is not a handy way for the time being. After some trials, laser induced X-ray radiograph is under investigation (see Fig. 9). Figure 10 shows the obtained radiography images with X-ray produced by irradiation of targets of Zr and Ag, where Zr seems to be better because of the X-ray energy just below the K-shell absorption edge of the Nb. Further study is needed for better visibility and practical applications.

## LOCAL REPAIR TECHNIQUE

Using the inspection devices, defects on the surfaces can be identified and analyzed. For those defects judged as harmful, the local repair technique can be applied. Several cavities have been already repaired and show satisfactory results (see Fig. 11). The micro-grinder can be inserted into the cavity, while the grinding head is retracted. After its positioning, some amount of water is applied to the area and the head with abrasives can start to grind. Additional EP and following processes are applied to the treated cavity to bring the cavity back to the line [7]. Figure 12 shows a recent design of the system, which has more powerful motor for the grinding.

## REFERENCES

- [1] Y. Iwashita, Y. Tajima, H. Hayano, Development of High Resolution Camera for Observations of Superconducting Cavities, Phys. Rev. ST Accel. Beams, 11, [093501-1]-[093501-6], 2008
- [2] A. Brinkmann, W. Singer, Nondestructive Testing of Niobium Sheets for SRF Cavities Using Eddy-Current and Squid Flaw Detection, Proc. LINAC08, Victoria, BC, Canada, pp.800-801
- [3] L. Cooley, C. Antoine, G. Wu, D. Sergatskov, H. Jiang, R. Schuessler, O. Frianeza, Fermilab QA and QC activities, FNAL slides for TTC meeting Jan 2008
- [4] Balle, Ch., Casas-Cubillos, J. et al, Influence of Thermal Cycling on Cryogenics Thermometers in Advances in Cryogenic Engineering 45B, Plenum, New York, 1999, pp. 1817.
- [5] H. Tongu, et al., Multipoint T-maps for Vertical Test of the Superconducting Accelerator Tubes, Proc. of the 6th Annual Meeting of Particle Accelerator Society of Japan, (2009) 409-411.
- [6] A. Canabal, et al., Development of a Temperature Mapping System for 1.3-GHz 9-Cell SRF Cavities, Proc. PAC07 2406 - 2408 (2007).
- [7] Updates on R&D of Non-destructive Inspection Systems for SRF Cavities, Y. Iwashita, H. Tongu, H. Hayano, T. Saeki, K. Watanabe, Proc. of SRF11, Chicago. Pp.447-449 (2011)

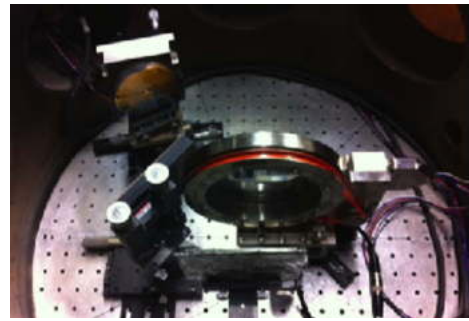


Figure 9: Layout for the laser induced X-ray radiography experiment. Various target materials can be irradiated by the laser to generate X-rays.

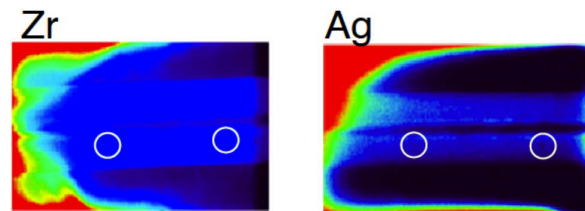


Figure 10: Obtained radiography images for targets of Zr and Ag. Both target materials give better visibility for the defects (sputter balls on the surface).

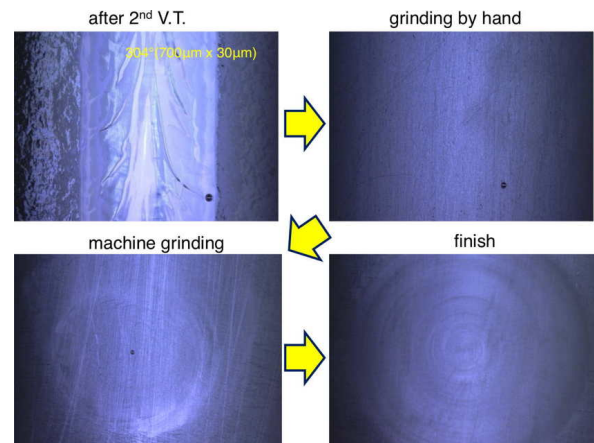


Figure 11: The progresses on the local grinding effect. The defect detected by the optical inspection was removed by the treatment.

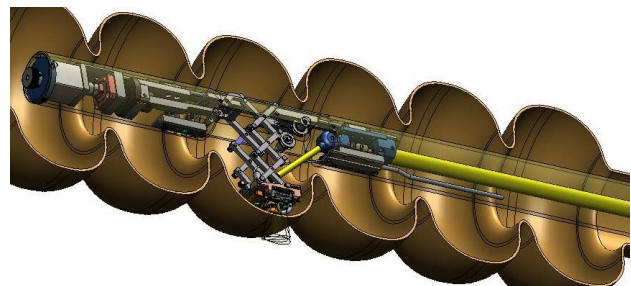


Figure 12: The grinding head assembly with a tiny monitoring camera protrudes towards the area to be treated. A powerful grinding motor located externally can reduce the processing time in this design.